

Blockade of glutamatergic and GABAergic receptor channels by trimethyltin chloride

^{1,3}Katharina Krüger, ^{1,3}Victoria Diepgrond, ^{1,3}Maria Ahnefeld, ^{1,3}Christina Wackerbeck, ¹Michael Madeja, ²Norbert Binding & ^{*,1}Ulrich Musshoff

¹Institute of Physiology I, Robert-Koch-Str. 27a, 48149 Münster, Germany and ²Institute of Occupational Medicine, University of Münster, Münster, Germany

1 Organotin compounds such as trimethyltin chloride (TMT) are among the most toxic of the organometallics. As their main target for toxicity is the central nervous system, the aim of the present study was to investigate the effects of TMT on receptor channels involved in various processes of synaptic transmission.

2 The *Xenopus* oocyte expression system was chosen for direct assessment of TMT effects on voltage-operated potassium channels and glutamatergic and GABAergic receptors, and hippocampal slices from rat brain for analyzing TMT effects on identified synaptic sites.

3 TMT was found to be ineffective, at $100 \mu\text{mol l}^{-1}$, against several potassium- and sodium-operated ion channel functions as well as the metabotropic glutamate receptor.

4 The functions of the ionotropic glutamate and the GABA_A receptor channels were inhibited by TMT in micromolar concentrations. Thus, at a maximum concentration of $100 \mu\text{mol l}^{-1}$, around 20–30% of the α -amino-3-hydroxy-5-methylisoxazole-4-propionic acid and GABA_A receptor-mediated ion currents and 35% of the *N*-methyl-D-aspartate receptor-mediated ion currents were blocked.

5 In the hippocampal slice model, the inhibitory effects of TMT were much stronger than expected from the results on the ion channels. Bath application of TMT significantly reduced the amplitudes of evoked excitatory postsynaptic field potentials in a concentration-dependent and nonreversible manner.

6 Induction of long-term potentiation, recorded from the CA1 dendritic region, was inhibited by TMT and failed completely at a concentration of $10 \mu\text{mol l}^{-1}$.

7 In general, TMT affects the excitatory and inhibitory synaptic processes in a receptor specific manner and is able to disturb the activity within a neuronal network.

British Journal of Pharmacology (2005) **144**, 283–292. doi:10.1038/sj.bjp.0706083

Published online 10 January 2005

Keywords: *Xenopus* oocyte; hippocampal slice; membrane currents; glutamate receptors; GABA receptors; potassium channels; organotin; trimethyltin

Abbreviations: ACSF, artificial cerebrospinal fluid; APV, 2-amino-5-phosphonovaleric acid; CNQX, 6-cyano-7-nitroquinoxaline-2,3-dione; DMSO, dimethyl sulfoxide; fEPSPs, evoked excitatory postsynaptic field potentials; KA, kainate; LTP, long-term potentiation; mGluR, metabotropic glutamate receptor; QUIS, quisqualate; TMT, trimethyltin chloride

Introduction

Contamination of the environment with organometallic compounds is a result of their widespread use, for example, as preservatives, biocides and antifouling paints, or by their natural formation *via* biomethylation of inorganic substrates (Thayer, 1995; Appel *et al.*, 2000; Craig *et al.*, 2003). Many of the organometallic compounds found in the environment are known to be highly toxic and especially neurotoxic (Craig *et al.*, 2003), thus representing a considerable environmental health hazard. This is especially true of organotin compounds such as trimethyltin chloride (TMT), which is among the most toxic of the organometallics (Snoeijs *et al.*, 1987; Cima *et al.*, 2003). Due to their high toxicity, TMT compounds are no

longer produced on an industrial scale. Nevertheless, they are detected for example in water and in waste deposit gas (Feldmann *et al.*, 1994). It is suggested that environmental methylated tin species are mostly formed by biomethylation (Cima *et al.*, 2003).

The main target of TMT toxicity is the central nervous system (CNS). Symptoms like decreased hearing, restlessness, psychomotor agitation, ataxia, confusion, disorientation, disturbances of short-term memory, amnesia, as well as partial or generalized seizures are reported after accidental intoxications (Besser *et al.*, 1987; Saary & House, 2002). TMT is known from animal experiments to accumulate in the CNS, resulting in pathological damage characterized by neuronal destruction, predominantly in the hippocampus and the cerebral cortex (Aschner & Aschner, 1992). Neurobehavioral alterations and impaired learning and performance are the

*Author for correspondence; E-mail: musshoff@uni-muenster.de

³These authors contributed equally to this work.

Published online 10 January 2005

result of TMT exposure of rats and are attributed to neuronal cell death (Reiter & Ruppert, 1984; Stanton *et al.*, 1991; Moser, 1996).

Despite these findings, the mechanisms involved in TMT-induced neuronal damage and in the neurotoxic symptoms observed are still not completely understood. Although neuronal cell death has, up to now, been the explanation for all observed effects, functional changes in the elemental processes of reception, conduction and transmission of bioelectrical signals might also contribute to TMT neurotoxicity and in particular to the impairment of learning and memory.

The aim of the present study was to investigate the effects of TMT on receptor channels involved in a variety of processes of synaptic transmission. For this purpose, we chose the *Xenopus* oocyte expression system for direct assessment of TMT effects on voltage- and ligand-operated ion channels, and hippocampal slices from rat brain for analyzing TMT effects on transmission at identified synaptic sites. The experiments were focused on glutamate receptors of the α -amino-3-hydroxy-5-methylisoxazole-4-propionic acid (AMPA) and *N*-methyl-D-aspartate (NMDA) type and on GABA receptors of the GABA_A type. Potassium channels were also studied, since the clinical signs of poisoning with metalloid compounds or metal ions include an increase of excitation, which would be in line with a blockade of potassium currents.

Methods

Electrophysiological studies on oocytes of Xenopus laevis

Preparation and injection of oocytes: The effects of TMT were tested on ligand- and voltage-operated ion channels from rat brain heterologously expressed in *Xenopus* oocytes. The technique for preparation and injection of oocytes has been described in detail elsewhere (Madeja *et al.*, 1997). Briefly, female *X. laevis* frogs were anesthetized by submersion in an ethyl-*m*-aminobenzoate solution (Sigma-Aldrich Chemie GmbH, Steinheim, Germany) and small sections of the ovary were removed surgically. Stage V or VI oocytes (Dumont, 1972) were isolated manually from the ovary and injected with mRNA or cRNA. The respective RNA was dissolved in distilled water and the solution was loaded into a glass capillary (tip diameter: 10 μ m) by suction. The mRNA was injected in aliquots of maximally 50 nl (50 ng RNA) per oocyte. The injected oocytes were maintained under sterile conditions at 20°C in a solution composed of (in mmol l⁻¹) NaCl 88, CaCl₂ 1.5, KCl 1, NaHCO₃ 2.4, MgSO₄ 0.8 and HEPES 5, pH 7.4, supplemented with penicillin (100 IU ml⁻¹) and streptomycin (100 μ g ml⁻¹). Every second day, the culture solution was exchanged and damaged oocytes were removed. Under these conditions, oocytes could be stored for 7–12 days after injection. Cloned voltage-operated potassium channels were expressed after injection of cRNA for the potassium channels Kv1.1, Kv1.2, Kv2.1 or Kv3.1. The cDNA encoding for the channel subunits was transcribed to cRNA using a commercial kit (mMessage mMachine™, Ambion, Austin, TX, U.S.A.) and T7 RNA polymerase. Denaturing agarose gel electrophoresis was used to check the quality of the cRNA product of each reaction and to quantify the yield. Ligand-operated ion channels were expressed in *Xenopus* oocytes after

injection of mRNA derived from rat brain after the method described by Cathala *et al.* (1983).

Application of TMT and the receptor agonists: For the experiments, an application setup was used that allows rapid solution exchange during electrophysiological measurements (Madeja *et al.*, 1991; 1995) and is based on the principle of the concentration clamp technique after Akaike *et al.* (1986). The solution surrounding the oocyte was exchanged by applying a negative pressure of 10 kPa. About 90% of the solution was exchanged in less than 10 ms with a fluid stream velocity of about 0.2 ms⁻¹. There was no fluid stream of the solution during the remaining time of the experiment. The control bath fluid was a Ringer solution composed of (in mmol l⁻¹) NaCl 115, KCl 2, CaCl₂ 1.8 and HEPES 10, pH 7.2. A stock solution of 200 μ mol l⁻¹ TMT (Merck, Darmstadt, Germany) was prepared in this Ringer solution, supplemented with 0.2% dimethyl sulfoxide (DMSO; Sigma-Aldrich Chemie GmbH, Steinheim, Germany) and kept at 4°C in glass bottles. TMT was added to the bath solution in concentrations of 0.1, 1, 10 and 100 μ mol l⁻¹. The different subtypes of glutamate-operated ion channels could be selectively activated by their specific agonists. NMDA (RBI, Research Biochemical International, Natick, U.S.A.) activates the NMDA receptors, kainate (KA; Sigma-Aldrich Chemie GmbH, Steinheim, Germany) activates the AMPA receptors, quisqualate (QUIS; Tocris, Bristol, U.K.) activates the metabotropic glutamate receptors (mGluRs), and γ -aminobutyric acid (GABA; Sigma-Aldrich Chemie GmbH, Steinheim, Germany) activates the GABA_A receptors. The concentrations of the receptor agonists used in these experiments have been selected on the basis of previous work and are in a common range for oocyte experiments (Bloms-Funke *et al.*, 1994; 1996; Montag *et al.*, 2004; Musshoff *et al.*, 1995; 1999). The concentrations of the tested ligands were (in μ mol l⁻¹): KA 50 or 100, NMDA 100 + glycine 10 (Sigma-Aldrich Chemie GmbH, Steinheim, Germany), QUIS 10 and GABA 50 or 100. The concentration of 100 μ mol l⁻¹ for KA, NMDA and GABA produces nearly maximal current responses. However, there was no difference in the effects of TMT using the different agonist concentrations.

Experimental protocol and analyses for voltage-operated channels: The activity of voltage-operated potassium channels was recorded at days 3 and 4 after injection of cRNA. The holding potential was -80 mV and command potentials were applied up to a potential of +60 mV. TMT was applied at least 30 s before eliciting potassium currents. Experiments using metalloid compounds with much longer preapplication times did not yield larger effects. Results were obtained from 48 defolliculated oocytes. The membrane currents were recorded and analyzed with a personal computer using commercial software (pClamp program, Axon Instruments Inc., Foster City, MI, U.S.A.), low-pass filtered at 1 kHz and corrected for leakage using a p/-4 pulse protocol. The current amplitude was measured at the peak current obtained during the depolarizing voltage step. Conductance-voltage relations of potassium channels were obtained by normalizing the conductance data to the maximal value under control conditions and by fitting the data to the Boltzmann equation $y = G_{\max} / (1 + \exp((V_{1/2} - V) / b))$ where y is the normalized conductance, G_{\max} is the normalized maximal conductance, $V_{1/2}$ is the potential of the half-maximal conductance, V is the voltage and b is the slope factor.

Experimental protocol and analyses for ligand-operated channels: The activity of ligand-operated channels was examined from day 3 to 12 after injection of poly(A)+/-RNA by measuring transmembranous ion currents through the different receptor channels types, triggered by bath application of the various specific agonists. For this purpose, the oocytes were voltage clamped at -50 or -70 mV with microelectrodes filled with 2 M KCl to give electrode resistances of 1–2 M Ω . The results were obtained from 110 oocytes of 24 donors with membrane resistances of 0.3–1.6 M Ω . TMT and the receptor agonists were applied to the oocytes for 60 s. Since repeated application of the glutamate and GABA receptor agonists with short recovery periods led to a gradual decline in responsiveness of the oocytes, we left 10–15 min between each application. The receptor agonists were initially administered separately to the oocyte and then, after a latency of 10–15 min, simultaneously with TMT, beginning with the lowest TMT concentration (0.1 $\mu\text{mol l}^{-1}$). Subsequently, the tested ligand was again administered separately. If this second agonist control response did not differ by more than 15% (corresponding to the maximal s.d. in the variance of subsequently applied controls) from the first one, measurements were continued at the same oocyte and TMT was again administered simultaneously with the agonist (with increasing TMT concentrations of 1, 10 and 100 $\mu\text{mol l}^{-1}$). If the subsequent control reaction differed by more than 15% from the first control reaction, the measurements were discontinued at that oocyte. The membrane currents were recorded and analyzed with a personal computer using custom-designed modified software. For analysis of possible effects of TMT on the ligand-operated receptor channel functions, the amplitudes of all membrane currents were measured 2 s before termination of substance application. The amplitude of each coapplication of TMT and agonist was normalized to the directly preceding control reaction (i.e. application of the agonist alone). The significance of the differences was calculated using the paired *t*-test. Values were considered significantly different if $P \leq 0.05$. Mean values and s.e.m. of membrane currents were additionally determined separately for each of the tested TMT concentrations. For the administration of QUIS, we used a modified protocol, since administration of QUIS activates oscillatory calcium-activated chloride currents in voltage-clamped oocytes (cf. Montag *et al.*, 2004) and oocytes showed a strong intra- and interindividual variability in their responses. Repetitive activation of the mGluR showed a constant desensitization of the responses, even when the delay between the consecutive applications was prolonged to 30 min. For this reason, TMT was applied 60 s after the first activation of the mGluR by QUIS for 30 s simultaneously with QUIS. Because of the strong oscillatory component of the mGluR responses, an analysis of amplitudes was not possible; for this reason, we compared the response areas 30 s before and 30 s after application of TMT using custom-designed modified software.

Electrophysiological studies on hippocampal slices from rats

Preparation of hippocampal slices: The technique for slice preparation of hippocampal tissue has been described in detail elsewhere (Musshoff *et al.*, 2002). Briefly, the brain tissue of rats (190–340 g, 2–4 months old) of both sexes was removed

under ether anesthesia. Both hippocampi were excised free from the brain and submerged in chilled ($2-4^{\circ}\text{C}$) artificial cerebrospinal fluid (ACSF) for about 1 min. Slices of 500 μm thickness from the dorsal hippocampus were cut by means of a McIlwain tissue chopper. The slices were preincubated in a submersion chamber for at least 60 min in ACSF at 28°C . After 30 min, the CaCl_2 concentration was raised from 1 to 2 mmol l^{-1} . The ACSF contained (in mmol l^{-1}) NaCl 124, KCl 4, CaCl_2 2, NaH_2PO_4 1.24, NaHCO_3 26, MgCl_2 1.3 and glucose 10, and was constantly bubbled with 95% O_2 and 5% CO_2 to maintain a pH of 7.4. For electrophysiological investigations, slices were maintained in a submerged type recording chamber with temperature (32°C), pH (7.4) and flow rate (4 ml min^{-1} , bath volume 1 ml) of ACSF being continuously monitored. The stock solution of TMT (200 $\mu\text{mol l}^{-1}$ TMT in ACSF with DMSO at a concentration of 0.1%) was diluted immediately prior to experiments at the concentrations indicated.

Induction of excitatory postsynaptic potentials: Excitatory postsynaptic potentials (EPSPs) were elicited by Schaffer collateral stimulation through a bipolar stimulation electrode and recorded as extracellular field potentials with ACSF-filled glass recording electrodes (0.5–1.5 M Ω) placed in the stratum radiatum of the CA1 region. Only synaptic potentials without superimposed population spikes were used for the experiments. For slices judged to be healthy, the synaptic response to a standard test stimulus (0.033 Hz) was monitored until a stable recording was obtained, and the input–output relationship was then determined. From this relationship, the stimulus strength producing a response of approximately 50% of the maximal response amplitude was determined and used for all subsequent experiments. After stable baseline recordings of the responses for 20 min, TMT was bath-applied to the hippocampal slices and the effects were monitored for a further 60–90 min. To evaluate the involvement and fraction of AMPA and NMDA receptors in the evoked excitatory postsynaptic field potential (fEPSP), the AMPA receptor antagonist 6-cyano-7-nitroquinoxaline-2,3-dione (CNQX, 50 $\mu\text{mol l}^{-1}$) and the NMDA receptor antagonist 2-amino-5-phosphonovaleric acid (APV, 50 $\mu\text{mol l}^{-1}$) were added to the bathing solution.

Induction of long-term potentiation: The baseline presynaptic stimulation was delivered at 0.033 Hz for 20 min using a stimulation intensity evoking approximately 50% of maximal postsynaptic responses. Following the application of the high-frequency stimulus (3×100 Hz, 1 s duration, intertrial interval 10 s), stimulation was again delivered at 0.033 Hz but now resulted in a potentiated synaptic response, which was recorded for a further 60–90 min. TMT was bath-applied to the hippocampal slices 15 min before long-term potentiation (LTP) induction and washed out 5 min after setting of the high-frequency stimulus. To evaluate the involvement of NMDA receptors in the induction of LTP, the NMDA receptor antagonist APV (50 $\mu\text{mol l}^{-1}$) was added to the bathing solution.

Analyses: The evoked synaptic responses were recorded and analyzed with a personal computer using custom-developed software (LTP program, version 2.30D; Anderson & Collingridge, 2001) and a digital oscilloscope. The field EPSPs were quantified by measurements of various parameters, including the slope and amplitude of the synaptic responses. Since the results obtained were generally consistent across the parameters, only the values for the amplitude are shown. Each

amplitude of EPSP under TMT application was normalized to the average amplitude of 10 min baseline recordings of the EPSPs acquired before TMT application. For LTP experiments, the amplitudes of the post-tetanic responses were normalized to the average of 10 min baseline responses. In addition, the data were grouped into 10 min bins. The significance of the differences between the means was calculated using a one-way analysis of variance (ANOVA) with Dunn's method. Values were considered significantly different if $P \leq 0.05$. In the text, values are shown as mean \pm s.e.m.

Results

X. laevis oocytes

Voltage-operated ion channels *Effects of TMT on voltage-operated potassium channels:* The Kv channels yielded potassium currents in the μ A range with positive going potential steps. For example, potassium currents of the Kv2.1 channel were found to be positive to -30 mV. The currents increased relatively slowly and did not inactivate significantly during the 500 ms test pulses (Figure 1a). Due to the extracellular potassium concentration of 2 mmol l^{-1} and the intracellular concentration of $75\text{--}80 \text{ mmol l}^{-1}$ (cf. Bloms *et al.*, 1993), the potassium equilibrium of the oocytes can be assumed to be around -90 mV after estimation with the Nernst equation. Since the holding potential of -80 mV was close to this equilibrium potential, potassium tail currents were very small and outward directed. The application of TMT, even at concentrations of $100 \mu\text{mol l}^{-1}$, however, did not alter the potassium currents significantly (Figure 1b). In Table 1, the mean results with $100 \mu\text{mol l}^{-1}$ TMT are shown for the four tested channels. For all channels, the mean decrease in maximum conductance was less than 5% of control and the mean shift of the potential of half-maximum conductance was less than 2 mV. Experiments with TMT concentrations of 1 and $10 \mu\text{mol l}^{-1}$ yielded even smaller effects (data not shown).

In pilot experiments, we tested the effect on a neuronal sodium channel (rBII). However, in these experiments, also after application of $100 \mu\text{mol l}^{-1}$ TMT, the change in current was below 5% at every tested potential in the range of -80 to $+40$ mV ($n=4$, data not shown).

Ligand-operated ion channels *Control experiments:* Oocyte currents induced by application of glutamatergic agonists (NMDA, KA, QUIS) and GABA are exclusively elicited by heterogeneously expressed receptors after injection of mRNA

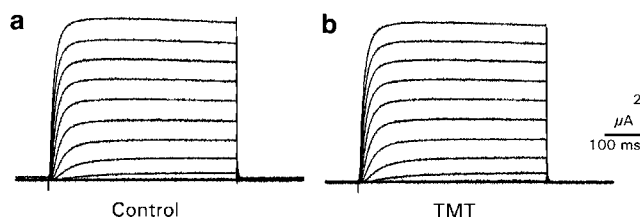


Figure 1 Effects of TMT on Kv2.1 potassium currents. Potential steps from -80 to $+60$ mV under control conditions (CTRL) (a) and with $100 \mu\text{mol l}^{-1}$ TMT (b). Original recordings.

Table 1 Effects of TMT ($100 \mu\text{mol l}^{-1}$) on currents of four Kv potassium channels

Channel	$G_{\text{maxTEST}}/G_{\text{maxCTRL}}$	$V_{1/2\text{CTRL}} - V_{1/2\text{TEST}}$	$\text{slope}_{\text{TEST}}/\text{slope}_{\text{CTRL}}$	n
Kv1.1	0.97 ± 0.01	-1.9 ± 1.1 mV	0.97 ± 0.02	4
Kv1.2	0.96 ± 0.01	$+1.1 \pm 0.4$ mV	1.02 ± 0.01	4
Kv2.1	0.97 ± 0.01	-0.3 ± 0.8 mV	1.00 ± 0.01	4
Kv3.1	0.96 ± 0.01	$+0.8 \pm 0.2$ mV	1.00 ± 0.00	4

In this table, the effects of TMT are expressed as changes in three variables: G_{max} , $V_{1/2}$ and slope. G_{max} is the maximal conductance, $V_{1/2}$ the potential of half-maximal conductance and slope, the slope of conductance. In each case, the results after with TMT treatment (TEST) are compared with results under control (CTRL) conditions, as shown. TMT did not significantly change any of the variables for any of the four K channels studied. The values of these variables are given as mean \pm s.e.m. for $n=4$ experiments for each channel.

from rat brain, since native oocytes show no responses to the application of these agonists (cf. Musshoff *et al.*, 2002). Furthermore, the specificity of the agonist-induced responses has been tested in previous experiments by blockade with selective antagonists (Musshoff *et al.*, 1995; 1999). The stability and reproducibility of the agonist-induced membrane currents had been tested in a series of control experiments for each receptor type. The receptors were activated by 6–9 successive applications of the agonist ($50 \mu\text{mol l}^{-1}$ KA, $100 \mu\text{mol l}^{-1}$ NMDA, $100 \mu\text{mol l}^{-1}$ GABA) for 60 s each and left for 10–15 min between applications. The results showed that the amplitude of the ion currents induced by a given concentration of an agonist could vary between individual oocytes, but was relatively stable and reproducible in a given oocyte. However, activation of the receptors showed a desensitization of the second response (e.g. a reduction in amplitude by approximately 20–25% in the case of the NMDA receptor), whereas the following responses were relatively stable compared to the second response. Therefore, the amplitude of the first application was generally discarded, the second one was taken as 100% and the following ones were normalized to this second response. Using this protocol, the subsequent responses of the AMPA receptors showed an average variance of maximal $5 \pm 12\%$ s.d. compared to the second responses ($n=15$; data not shown), the responses of the NMDA receptors showed an average variance of $6 \pm 15\%$ s.d. ($n=18$; data not shown) and those of the GABA receptors of $5 \pm 12\%$ s.d. compared to the second responses ($n=8$; data not shown).

To investigate the effect of the solvent on the receptor function, DMSO was administered at a concentration of 0.1% together with the different receptor agonists and normalized to the preceding control (agonist without DMSO). We found no significant effects of DMSO on AMPA receptor currents ($99.8 \pm 1.9\%$, $n=5$), on NMDA receptor currents ($99.5 \pm 8.2\%$, $n=7$) or on GABA receptor currents ($100.9 \pm 2.2\%$, $n=5$).

The effects of TMT on the membrane currents of the voltage-clamped oocytes were tested in 59 oocytes for concentrations of $0.0001\text{--}100 \mu\text{mol l}^{-1}$ TMT (i.e. without coapplication of the receptor agonists). In most cases, TMT had no effect ($n=45$), but in some cases, especially at a concentration of $100 \mu\text{mol l}^{-1}$, it caused an inward current of

maximal 29 nA ($n=29$) and occasionally outward currents with maximal amplitudes of 5 nA ($n=20$). Overall, in the range of 0.0001 – $10 \mu\text{mol l}^{-1}$ TMT, we found mean variations of 0.5 nA. For $100 \mu\text{mol l}^{-1}$ TMT, we found a mean membrane current of 3.7 ± 1.4 nA ($n=25$). These effects of TMT on membrane currents were accounted for in the analysis of the effects of TMT on the agonist-induced membrane currents by subtraction.

Effects of TMT on AMPA receptors: The effects of TMT on the AMPA-mediated membrane currents are shown in Figure 2a. The application of $50 \mu\text{mol l}^{-1}$ of the receptor agonist (white bars) elicited inward currents, which were reduced by coapplication of the agonist with $100 \mu\text{mol l}^{-1}$

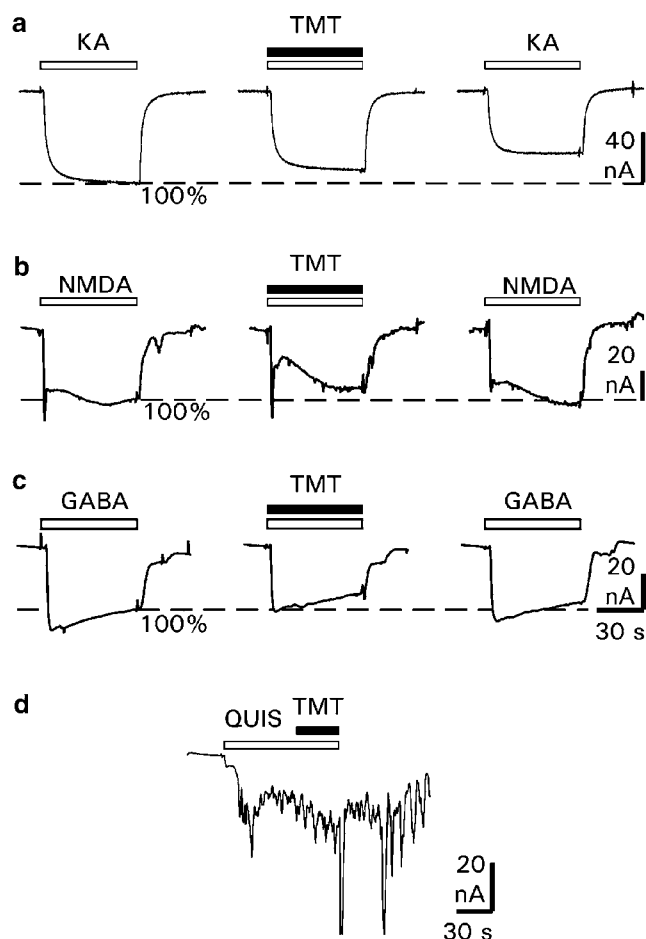


Figure 2 Effects of TMT on membrane currents elicited by the glutamate receptor agonists KA, NMDA and QUIIS, and by GABA. Original recordings of receptor-mediated membrane currents from single oocytes (a) with application of $50 \mu\text{mol l}^{-1}$ KA (left trace), with coapplication of $50 \mu\text{mol l}^{-1}$ KA and $100 \mu\text{mol l}^{-1}$ TMT (middle trace), and with control application of $50 \mu\text{mol l}^{-1}$ KA after TMT washout of 15 min (right trace); (b) with application of $100 \mu\text{mol l}^{-1}$ NMDA (left trace), with coapplication of $100 \mu\text{mol l}^{-1}$ NMDA and $100 \mu\text{mol l}^{-1}$ TMT (middle trace) and with control application of $100 \mu\text{mol l}^{-1}$ NMDA after TMT washout of 20 min (right trace); (c) with application of $100 \mu\text{mol l}^{-1}$ GABA (left trace), with coapplication of $100 \mu\text{mol l}^{-1}$ GABA and $100 \mu\text{mol l}^{-1}$ TMT (middle trace), and with control application of $100 \mu\text{mol l}^{-1}$ GABA after TMT washout of 15 min (right trace); (d) with application of $10 \mu\text{mol l}^{-1}$ QUIIS and coapplication of $10 \mu\text{mol l}^{-1}$ QUIIS and $10 \mu\text{mol l}^{-1}$ TMT. Delay between the applications: 10 min (a), 15 min (b, c). Horizontal bars mark the time of agonist applications (white) and TMT (black). Holding potential: -70 mV. Inward current: downward deflection.

TMT (black bar). Figure 3a summarizes all experiments and shows the relative blockade of the AMPA receptor-mediated responses. On average, TMT reduced receptor currents by 5–20% in a concentration-dependent manner. However, these reductions were significant only for concentrations of 1, 10 and $100 \mu\text{mol l}^{-1}$ TMT ($0.1 \mu\text{mol l}^{-1}$: $P=0.238$; $1 \mu\text{mol l}^{-1}$: $P=0.045$; $10 \mu\text{mol l}^{-1}$: $P=0.022$; $100 \mu\text{mol l}^{-1}$: $P=0.031$). The effects of TMT seem to be irreversible, since washout (15 min, $n=5$) of the organotin compound did not fully restore the receptor responses (Figure 2a, last trace).

Effects of TMT on NMDA receptors: The effects of TMT on the NMDA-induced membrane currents are shown in Figure 2b with original recordings from single oocytes after application of NMDA and after simultaneous application of NMDA and TMT. The application of $100 \mu\text{mol l}^{-1}$ NMDA (white bars) elicited inward currents, which were reduced by coapplication of NMDA with $100 \mu\text{mol l}^{-1}$ TMT (black bar). Figure 3b summarizes all experiments and shows the relative blockade of the NMDA-induced responses. On average, the NMDA-induced inward currents were concentration-dependently reduced by TMT by 4–35%. These reductions were significant for concentrations of 1, 10 and $100 \mu\text{mol l}^{-1}$ TMT ($0.1 \mu\text{mol l}^{-1}$: $P=0.726$; $0.5 \mu\text{mol l}^{-1}$: $P=0.913$; $1 \mu\text{mol l}^{-1}$:

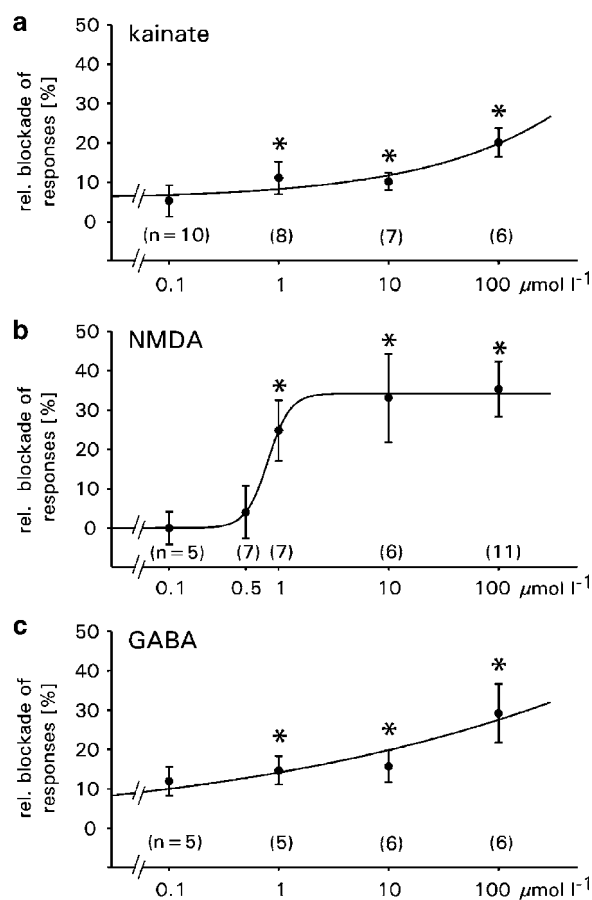


Figure 3 Effects of TMT on membrane currents through glutamate and GABA receptor channels in oocytes. Values shown are the means \pm s.e.m. of the relative blockade of the (a) AMPA receptor-mediated, (b) NMDA receptor-mediated and (c) GABA receptor-mediated membrane currents induced by application of TMT at various concentrations. *Significant blockade ($P \leq 0.05$); number of oocytes are in brackets.

$P=0.031$; $10\ \mu\text{mol l}^{-1}$: $P=0.050$; $100\ \mu\text{mol l}^{-1}$: $P=0.002$). These effects seem to be reversible since washout (20 min, $n=20$; 35 min, $n=4$) of TMT fully restored the NMDA responses (Figure 2b, last trace).

Effects of TMT on mGluRs: The effect of TMT on mGluRs is shown in Figure 2d with an original recording from a single oocyte after application of QUIS and simultaneous application of QUIS and TMT. The application of $10\ \mu\text{mol l}^{-1}$ QUIS (white bar) elicited oscillatory responses, which were not affected by coapplication of QUIS with $10\ \mu\text{mol l}^{-1}$ TMT (black bar). The comparison of the response areas 30 s before and 30 s after application of TMT showed no effect of TMT on membrane currents elicited by the mGluRs ($n=6$, $P=0.925$, paired *t*-test).

Effects of TMT on GABA_A receptors: The effects of TMT on the GABA-induced membrane currents are shown in Figure 2c with original recordings from single oocytes after application of GABA and after simultaneous application of GABA and TMT. The application of $100\ \mu\text{mol l}^{-1}$ GABA (white bars) elicited inward currents, which were reduced by $100\ \mu\text{mol l}^{-1}$ TMT (black bar). Figure 3c summarizes all experiments and shows the relative blockade of the GABA-induced responses. On average, the GABA-induced inward currents were reduced by 12–29% in a concentration-dependent manner. These reductions were significant for concentrations of 1, 10 and $100\ \mu\text{mol l}^{-1}$ TMT ($0.1\ \mu\text{mol l}^{-1}$: $P=0.054$; $1\ \mu\text{mol l}^{-1}$: $P=0.025$; $10\ \mu\text{mol l}^{-1}$: $P=0.050$; $100\ \mu\text{mol l}^{-1}$: $P=0.007$). The blockade seems to be irreversible since GABA responses were not fully restored after washout (15 min, $n=14$) of TMT (Figure 2c, last trace).

Rat hippocampal slices

Effects of TMT on evoked postsynaptic field potentials: To test whether TMT affects the transmission at the Schaffer collateral–CA1 synapse, evoked fEPSPs were measured under control conditions (ACSF, supplemented with 0.005% DMSO) and by administration of 0.1, 1 and $10\ \mu\text{mol l}^{-1}$ TMT (in ACSF, supplemented with 0.005% DMSO) for 60–90 min. In control experiments, the AMPA receptor antagonist CNQX ($50\ \mu\text{mol l}^{-1}$; $n=4$; data not shown) and the NMDA receptor antagonist APV ($50\ \mu\text{mol l}^{-1}$; $n=5$; data not shown) were added to the bathing solution. With application of CNQX, the evoked fEPSP was completely suppressed, whereas the application of APV did not change fEPSP in amplitude. This indicates that the evoked fEPSP is mainly due to the actions of AMPA receptors. Typical recordings of evoked fEPSP from the CA1 dendritic region before and after application of TMT are shown in Figure 4a. Under control conditions, the amplitude of fEPSP remained stable for 30 min and then started to rise slightly. The average fEPSP amplitude was $110\pm 3\%$ of baseline (time point at which the response was nearly stable and set as baseline reference; $n=8$; Figure 5a). Bath application of TMT reduced the amplitudes of evoked fEPSPs in a concentration-dependent manner. The average amplitudes were $97\pm 2\%$ of baseline with $0.1\ \mu\text{mol l}^{-1}$ TMT ($n=7$), $71\pm 7\%$ with $1\ \mu\text{mol l}^{-1}$ TMT ($n=5$) and $41\pm 14\%$ of baseline with $10\ \mu\text{mol l}^{-1}$ TMT ($n=5$). The onset of the blocking effect varied with the concentration of TMT. The gradual reduction in the amplitude of fEPSPs reached plateau levels approximately 60–80 min following the application of TMT at concentrations of 0.1 and $1\ \mu\text{mol l}^{-1}$. After 60 min application of $10\ \mu\text{mol l}^{-1}$ TMT, the fEPSP

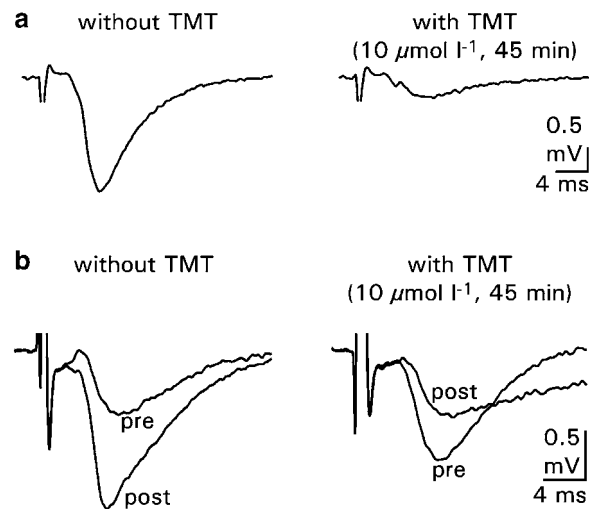


Figure 4 Effects of TMT on evoked postsynaptic potentials and LTP in hippocampal slice preparations. Typical traces of postsynaptic responses (fEPSPs) in the CA1 dendritic layer (a) after stimulation of the Schaffer collaterals without and with administration of $10\ \mu\text{mol l}^{-1}$ TMT, (b) before (pre) and after (post) high-frequency stimulation of the Schaffer collaterals; original recordings were without and with administration of $10\ \mu\text{mol l}^{-1}$ TMT.

responses were more or less depressed. The depressant effects were not reversible after a 30-min washout of TMT (Figure 5a). A comparison of the fEPSP amplitudes averaged into 10 min bins showed that the postsynaptic amplitudes were significantly reduced at concentrations of 1 and $10\ \mu\text{mol l}^{-1}$ TMT at most time points (Figure 5b). The effect of $0.1\ \mu\text{mol l}^{-1}$ TMT, however, became significant only after 30 min of bath application.

Effects of TMT on LTP: This set of experiments was designed to determine whether the induction of LTP, recorded from the CA1 dendritic region, is affected by TMT. In control experiments, the NMDA receptor antagonist APV ($50\ \mu\text{mol l}^{-1}$; $n=5$; data not shown) was added to the bathing solution. The application of APV prevents the induction of LTP, indicating that LTP at this type of synapse is mediated by NMDA receptors. Typical recordings of postsynaptic responses before and after application of the high-frequency stimulus train under control conditions and with TMT application are shown in Figure 4b. After a stable baseline, the slices were treated with TMT (0.1 , 1 and $10\ \mu\text{mol l}^{-1}$) for 20 min, and 5 min before washout of TMT, the LTP stimulus was applied. Overall, the magnitude of the enhancement of fEPSP was found to be reduced in slices treated with TMT compared to control slices. The blocking effects were reinforced with increasing concentrations of TMT, and at a concentration of $10\ \mu\text{mol l}^{-1}$, the postsynaptic potentiation failed (Figure 6a). The average fEPSP amplitude was $234\pm 2\%$ of baseline under control conditions ($n=7$), $213\pm 2\%$ of baseline with $0.1\ \mu\text{mol l}^{-1}$ TMT ($n=7$), $137\pm 3\%$ with $1\ \mu\text{mol l}^{-1}$ TMT ($n=6$) and $55\pm 6\%$ with $10\ \mu\text{mol l}^{-1}$ TMT ($n=6$). A comparison of the fEPSP amplitudes averaged into 10 min bins showed that the fEPSP amplitudes were significantly smaller in slices treated with TMT at concentrations of 1 and $10\ \mu\text{mol l}^{-1}$ (Figure 6b). The effect of $0.1\ \mu\text{mol l}^{-1}$ TMT, however, became inconsistently significant after 30 min of bath application. The inhibitory effect of TMT was partially reversible after washout of TMT for 60 min and setting a second LTP stimulus ($n=6$; data not shown).

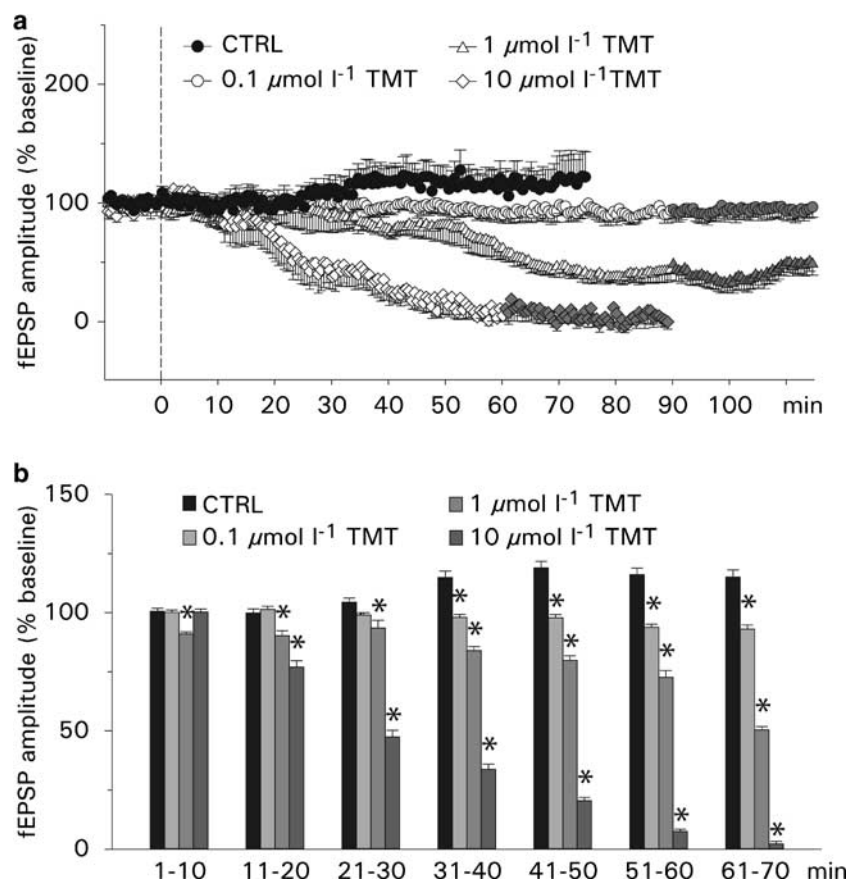


Figure 5 Effects of TMT on evoked postsynaptic potentials. (a) Values shown are the means \pm s.e.m. of the fEPSP amplitudes (normalized to the average of 10 min baseline responses) under control condition (without TMT) and after administration of TMT at various concentrations. TMT was given at time = 0 and washed out after 90 or 60 min (gray symbols). (b) Time course of effect of TMT on fEPSP. Means \pm s.e.m. of the fEPSP amplitudes were averaged into 10 min bins, starting at time = 0 (see panel a).

Discussion

Until now, few investigations have studied the influence of TMT on neuronal membrane properties and on the function of ion channels. The effect of TMT on voltage-gated potassium currents was investigated in lymphocytes and neuroblastoma cells: in contrast to tributyltin and triphenyltin, TMT did not affect the voltage-gated potassium currents (Oortgiesen *et al.*, 1996). A more recent paper reported that, in identified neurons of the mollusc *Lymnaea stagnalis*, voltage-activated sodium currents were only affected at a TMT concentration of $100 \mu\text{mol l}^{-1}$ (Györi *et al.*, 2000). Furthermore, in hippocampal CA1 neurons, TMT slowly depolarized the membrane potential, decreased action potential amplitudes and prolonged the duration of EPSPs (Harkins & Armstrong, 1992). Overall, due to the different cell systems and their distinct properties, these studies are fragmentary and have provided only restricted insights into the effect of TMT, at the level of ion channels. With the *Xenopus* oocyte expression system, we used a systematic approach to study direct effects of TMT on different voltage- and ligand-operated ion channels and, to verify our results, we extended our investigations to an established neuronal *in vitro* system, the hippocampal slice model. The principal finding of this study is that some of the neurotoxic effects of TMT are probably provoked by functional impairments of ligand-operated ion channels, in particular glutamatergic and GABAergic receptor channels.

Sensitivity of neuronal ion channels to TMT

The present experiments revealed that TMT, even at high concentrations, is ineffective against the metabotropic glutamate receptor, several mammalian potassium channels and the voltage-operated sodium channel, in line with the observations of Oortgiesen *et al.* (1996). However, the functions of the ionotropic glutamate and the GABA_A receptor channels were affected in an inhibitory manner by micromolar concentrations of TMT. Thus, at a maximum concentration of $100 \mu\text{mol l}^{-1}$, around 20–30% of the AMPA and GABA_A receptor-mediated ion currents and 35% of the NMDA receptor-mediated ion currents were blocked. With respect to the effects of TMT on receptor channels, it has to be borne in mind that the pharmacological sensitivity of channels expressed in oocytes is often reduced in comparison to mammalian cell lines (Madeja *et al.*, 2000; Rolfs *et al.*, 2000). Therefore, it is obvious that this expression system is not suitable for measuring *absolute* pharmacological values but that the oocyte is a useful tool for studies determining 'relative' values, for example, basic mechanisms of drug action. For these reasons, TMT can be assumed to have an even stronger effect on the receptor channels in neuronal cells than that on *Xenopus* oocytes reported in this study (see below).

As far as the site of action of TMT at ion channels is concerned, the results presented here are not decisive. It is generally accepted that an important neurotoxic site of

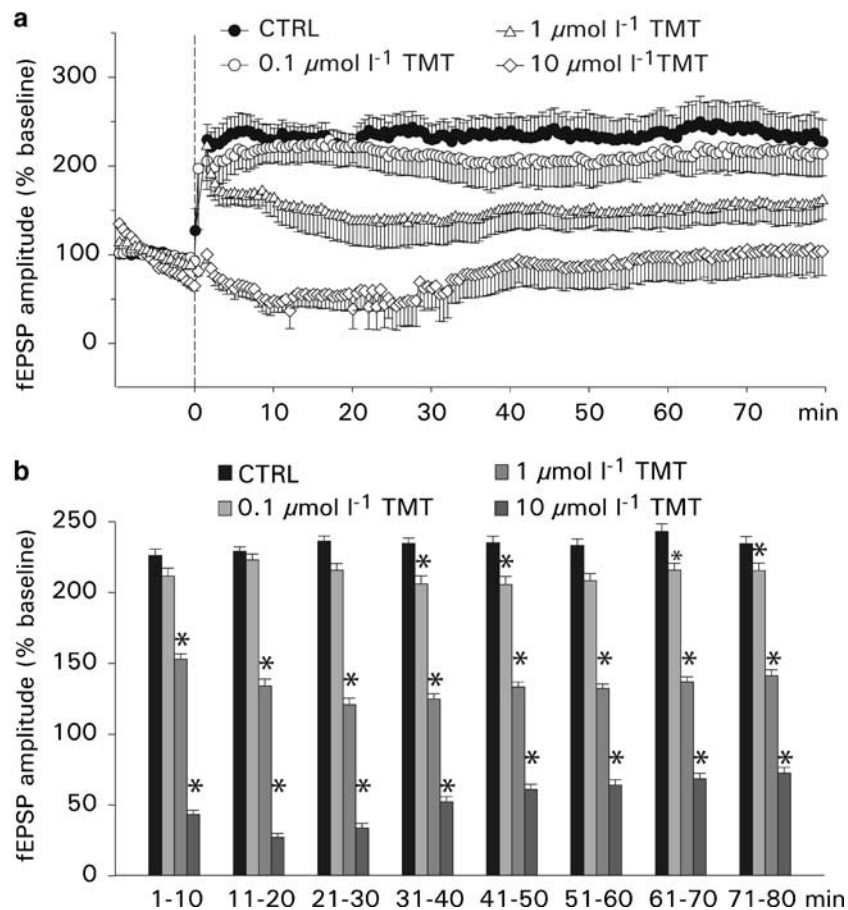


Figure 6 Effects of TMT on LTP. (a) Values shown are the means \pm s.e.m. of the fEPSP amplitudes (normalized to the average of 10 min baseline responses) under control condition (without TMT) and after administration of TMT at various concentrations. TMT was given 15 min before setting the LTP stimulus (time = 0) and washed out 5 min after the LTP stimulus. (b) Time course of effects of TMT on LTP. Here the means \pm s.e.m. of the fEPSP amplitudes are averaged into 10 min bins, starting at time = 0 (see panel a).

organotins, such as TMT, is the cell membrane (Aschner & Aschner, 1992; Richter-Landsberg & Besser, 1994). In line with this suggested neurotoxic site are the inhibitory effects on ion channels. However, since TMT selectively inhibits only a specific set of ligand-operated ion channels, it is likely that this compound interacts in a more specific way with these receptor channels and not *via* a general alteration of the neuronal membranes. Furthermore, the irreversibility of the effects, measured in the oocyte expression system as well as in the hippocampal slice model, may point to an action of TMT at a site within the membrane or on the intracellular side of the receptor channels. In this context, it also has to be borne in mind that local levels of TMT at or within the membrane may be much higher than the levels measured in the extracellular fluid (Aschner & Aschner, 1992).

Since TMT inhibits glutamatergic and GABAergic-operated ion channels, we propose that this organotin compound affects the neural transmission at the Schaffer collateral-CA1 synapse. In fact, the results obtained with the *Xenopus* system are fully compatible with the action of TMT on the synaptic process in hippocampal slices. However, the effects of TMT in slice experiments are surprisingly much stronger than expected from the results in oocytes, at the ion channel level. Although the blocking effects of $10 \mu\text{mol l}^{-1}$ TMT on the ionotropic glutamate and GABA receptors reached levels of only 10%

(AMPA receptor), 16% (GABA_A receptor) and 34% (NMDA receptor), the fEPSP in hippocampal slices was almost completely blocked after a 60 min application of TMT at this concentration. Furthermore, at a concentration of $1 \mu\text{mol l}^{-1}$ TMT, the fEPSP amplitude was reduced to about 50%, although in *Xenopus* oocytes the ligand-operated ion channels were only slightly affected at this concentration (AMPA receptor: 11%; GABA_A receptor: 14%; NMDA receptor: 25%). Similar inhibitory effects of TMT occurred after LTP at the Schaffer collateral-CA1 synapse, which is mainly conditioned by NMDA receptors. As expected from the blocking effects on the NMDA receptors, $1 \mu\text{mol l}^{-1}$ TMT reduced the high-frequency stimulus-evoked potentiation to approximately 50% of the control value and $10 \mu\text{mol l}^{-1}$ TMT completely eliminated LTP.

Three mechanisms may be suggested to explain this elevated sensitivity of TMT in the hippocampal slice model: firstly, an additive reaction of the inhibitory effects of TMT on the diverse ion channels; secondly, a possible accumulation of the toxic substance within the membranes and cells of the hippocampus (Aschner & Aschner, 1992); and thirdly, a reduced pharmacological sensitivity of the heterologously expressed channels in oocytes, leading to an underestimation of the effects. In any case, it is clear that TMT could act on a number of other receptors (adenosine, serotonin, etc.) or

voltage-activated ion channels not examined in our experiments. However, effects of TMT on voltage-operated calcium channels, which are common targets for metal ions, can be excluded, since $10 \mu\text{mol l}^{-1}$ TMT has no influence on calcium currents (Professor Büsselberg, University of Essen-Duisburg, Germany, personal communication). Additionally, it cannot be excluded that additional membrane or cytotoxic effects contributed to this inhibitory effect. For example, the known inhibitory effect of TMT on the Na^+/K^+ -ATPase activity may also slowly disturb neuronal activity and, particularly, the processes of the synaptic transmission (Aschner *et al.*, 1992).

Significance in TMT poisoning

Neurological effects of TMT were first reported in 1955 (Stoner *et al.*, 1955). It was more than 20 years later that the deleterious effects of TMT on the CNS were analyzed any further. Several investigators observed neuronal damage by TMT predominantly localized in the hippocampus, and also in the pyriform cortex, the amygdaloid nucleus, the brainstem, the neocortex and the spinal cord of rats (for an overview, see Snoeij *et al.*, 1987), demonstrating a high neurotoxic potential of this organotin compound (Richter-Landsberg & Besser, 1994; McCann *et al.*, 1996; Karpiaik & Eyer, 1999; Scallet *et al.*, 2000; Röhl *et al.*, 2001). In animal experiments, the neurobehavioral toxicity of TMT was investigated using different maze tests. Locomotor hyperactivity, aggressiveness as well as impaired learning, memory and performance have been reported after a single dose of TMT (Swartzwelder *et al.*, 1981; 1982; Walsh *et al.*, 1982; Reiter & Ruppert, 1984).

The goal of the present experiments was to analyze TMT-specific impairments of the synaptic transmission in a neuronal network. The results show that TMT affects the synaptic transmission in the CA1 region rapidly (within minutes) and

concentration-dependently. The inhibition of synaptic activity takes place at TMT concentrations comparable to those reported in brain, following *in vivo* exposure ($5\text{--}18.5 \mu\text{mol l}^{-1}$; cf. Aschner & Aschner, 1992). Since the toxicant in our experiments, was applied only for short time periods (20–90 min), the effects could be classified as acute and functional neurotoxic effects. Long-term effects of TMT are naturally not measurable with this organotypic *in vitro* preparation and it is doubtful whether TMT causes cell death in the short time used in the present experiments. A review of the relevant literature shows that TMT-induced neurodegeneration and cell loss have been found after exposure times of 16 h (Reuhl & Cranmer 1984), 1 day (e.g. Balaban *et al.*, 1988) or several days (e.g. Ishida *et al.*, 1997). However, the time course of degenerative changes, especially the beginning of neurodegeneration, has not been described adequately so far.

Although the clinical significance of our findings remains to be clarified, it can be assumed that, besides the well-known cytotoxic effects of TMT exposure, functional impairments of synaptic activity contribute to the neurotoxic signs. Of particular importance is the attenuation of NMDA responses and LTP. This effect of TMT has important implications for neuronal function and may explain the TMT-induced impairment of behavior patterns, in connection with learning and memory.

We are grateful to Professor Hirner, Dr L. Hartmann and J. Hippler, Institute for Environmental Analytical Chemistry, University of Duisburg-Essen, for helpful discussions and for supplying the TMT, to Dr P. Boerrigter for designing the application setup and providing the self-made custom-designed software, and to A. Markovic, S. Sasikanthan and I. Winkelhues for excellent technical assistance. This work was supported by Deutsche Forschungsgemeinschaft (DFG MA 1641/10-1, MU 1377/3-2, MU 1377/3-3).

References

- AKAIKE, N., INOUE, M. & KRISHTAL, O.A. (1986). Concentration clamp study of γ -aminobutyric acid-induced chloride current kinetics in frog sensory neurones. *J. Physiol.*, **379**, 171–185.
- ANDERSON, W.W. & COLLINGRIDGE, G.L. (2001). The LTP Program: a data acquisition program for on-line analysis of long-term potentiation and other synaptic events. *J. Neurosci. Methods*, **15**, 71–83.
- APPEL, K.E., BÖHME, C., PLATZEK, T., SCHMIDT, E. & STINCHCOMBE, S. (2000). Organozinnverbindungen in verbrauchernahen Produkten und Lebensmitteln. *Umweltmed. Forsch. Prax.*, **5**, 67–77.
- ASCHNER, M. & ASCHNER, J.L. (1992). Cellular and molecular effects of trimethyltin and triethyltin: relevance to organotin neurotoxicity. *Neurosci. Biobehav. Rev.*, **16**, 427–435.
- ASCHNER, M., GANNON, M. & KIMELBERG, H.K. (1992). Interactions of trimethyl tin (TMT) with rat primary astrocyte cultures: altered uptake and efflux of rubidium, L-glutamate and D-aspartate. *Brain Res.*, **582**, 181–185.
- BALABAN, C.D., O'CALLAGHAN, J.P. & BILLINGSLEY, M.L. (1988). Trimethyltin-induced neuronal damage in the rat brain: comparative studies using silver degeneration stains, immunocytochemistry and immunoassay for neuronotypic and gliotypic proteins. *Neuroscience*, **26**, 337–361.
- BESSER, R., KRÄMER, G., THÜMLER, R., BOHL, J., GUTMANN, L. & HOPF, H.C. (1987). Acute trimethyltin limbic-cerebellar syndrome. *Neurology*, **37**, 945–950.
- BLOMS, P., MUSSHOF, U., MADEJA, M., LEHMENKÜHLER, A., SPENER, F. & SPECKMANN, E.-J. (1993). Permeabilität der Plasmamembran von Oozyten (*Xenopus laevis*) für die epileptogene Substanz Pentylentetrazol. In: *Epilepsie.*, ed. Stefan, H. Vol. 92, pp. 378–382. Reinbeck: Einhorn Presse Verlag.
- BLOMS-FUNKE, P., MUSSHOF, U., MADEJA, M., SPENER, F. & SPECKMANN, E.-J. (1994). Decrease and increase of responses to glutamate receptor agonists in RNA-injected *Xenopus* oocytes by the epileptogenic agent pentylentetrazol: dependence on the agonist concentration. *Neurosci. Lett.*, **181**, 161–164.
- BLOMS-FUNKE, P., MADEJA, M., MUSSHOF, U. & SPECKMANN, E.-J. (1996). Effects of pentylentetrazol on GABA receptors expressed in *Xenopus* oocytes: extra- and intracellular sites of action. *Neurosci. Lett.*, **205**, 115–118.
- CATHALA, G., SAVOURET, J.-F., MENDEZ, B., WEST, B.L., KARIN, M., MARTIAL, J.A. & BAXTER, J.D. (1983). A method for isolation of intact translationally active ribonucleic acid. *DNA*, **2**, 329–335.
- CIMA, F., CRAIG, P.J. & HARRINGTON, C. (2003). Organotin compounds in the environment. In: *Organometallic Compounds in the Environment*, ed. Craig, P.J. pp. 101–149. Chichester: John Wiley & Sons Ltd.
- CRAIG, P.J., ENG, G. & JENKINS, R.O. (2003). Occurrence and pathways of organometallic compounds in the environment – general considerations. In: *Organometallic Compounds in the Environment*, ed. Craig, P.J. pp. 1–55. Chichester: John Wiley & Sons Ltd.
- DUMONT, J.N. (1972). Oogenesis in *Xenopus laevis* (Daudin) I. Stages of oocyte development in laboratory maintained animals. *J. Morphol.*, **136**, 153–180.
- FELDMANN, J., GRUMPING, R. & HIRNER, A.V. (1994). Determination of volatile metal and metalloids compounds in gases from domestic waste deposits with GC ICP-MS. *Fresen J. Anal. Chem.*, **350**, 228–234.
- GYÖRI, J., PLATOSHYN, O., CARPENTER, D.O. & SALANKI, J. (2000). Effect of inorganic and organic tin compounds on ACh- and voltage-activated Na currents. *Cell. Mol. Neurobiol.*, **20**, 591–604.

- HARKINS, A.B. & ARMSTRONG, D.L. (1992). Trimethyltin alters membrane properties of CA1 hippocampal neurons. *Neurotoxicology*, **13**, 569–582.
- ISHIDA, N., AKAIKE, M., TSUTSUMI, S., KANAI, H., MASUI, A., SADAMATSU, M., KURODA, Y., WATANABE, Y., MC EWEN, B.S. & KATO, N. (1997). Trimethyltin syndrome as a hippocampal degeneration model: temporal changes and neurochemical features of seizure susceptibility and learning impairment. *Neuroscience*, **81**, 1183–1191.
- KARPIAK, V.C. & EYER, C.L. (1999). Differential gliotoxicity of organotins. *Cell Biol. Toxicol.*, **15**, 261–268.
- MADEJA, M., MUSSHOF, U. & SPECKMANN, E.-J. (1991). A concentration-clamp system allowing two-electrode voltage-clamp investigations in oocytes of *Xenopus laevis*. *J. Neurosci. Methods*, **38**, 267–269.
- MADEJA, M., MUSSHOF, U. & SPECKMANN, E.-J. (1995). Improvement and testing of a concentration-clamp system for oocytes of *Xenopus laevis*. *J. Neurosci. Methods*, **63**, 211–213.
- MADEJA, M., MUSSHOF, U. & SPECKMANN, E.-J. (1997). Follicular tissues reduce drug effects on ion channels in oocytes of *Xenopus laevis*. *Eur. J. Neurosci.*, **9**, 599–604.
- MADEJA, M., MÜLLER, V., MUSSHOF, U. & SPECKMANN, E.-J. (2000). Sensitivity of native and cloned hippocampal delayed-rectifier potassium channels to verapamil. *Neuropharmacology*, **39**, 202–210.
- MCCANN, M.J., O'CALLAGHAN, J.P., MARTIN, P.M., BERTRAM, T. & STREIT, W.J. (1996). Differential activation of microglia and astrocytes following trimethyl tin-induced neurodegeneration. *Neuroscience*, **72**, 273–281.
- MONTAG, S., KRÜGER, K., MADEJA, M., SPECKMANN, E.-J. & MUSSHOF, U. (2004). Contribution of the cytoskeleton and the phospholipase C signaling pathway to fluid stream-induced membrane currents. *Cell Calcium*, **35**, 333–343.
- MOSER, V.C. (1996). Rat strain- and gender-related differences in neurobehavioral screening: acute trimethyltin neurotoxicity. *J. Toxicol. Environ. Health*, **47**, 567–586.
- MUSSHOF, U., MADEJA, M., BINDING, N., WITTING, U. & SPECKMANN, E.-J. (1995). Lead-induced blockade of kainate-sensitive receptor channels. *Naunyn-Schmiedeberg's Arch. Pharmacol.*, **353**, 42–45.
- MUSSHOF, U., MADEJA, M., BINDING, N., WITTING, U. & SPECKMANN, E.-J. (1999). Effects of 2-phenoxyethanol on *N*-methyl-D-aspartate (NMDA) receptor-mediated ion currents. *Arch. Toxicol.*, **73**, 55–59.
- MUSSHOF, U., RIEWENHERM, D., BERGER, E., FAUTECK, J.-D. & SPECKMANN, E.-J. (2002). Melatonin receptors in rat hippocampus: molecular and functional investigations. *Hippocampus*, **12**, 165–173.
- OORTGIESEN, M., VISSER, E., VIJVERBERG, H.P.M. & SEINEN, W. (1996). Differential effects of organotin compounds on voltage-gated potassium currents in lymphocytes and neuroblastoma cells. *Naunyn-Schmiedeberg's Arch. Pharmacol.*, **353**, 136–143.
- REITER, L.W. & RUPPERT, P.H. (1984). Behavioral toxicity of trialkyltin compounds: a review. *Neurotoxicology*, **5**, 177–186.
- REUHL, K.R. & CRANMER, J.M. (1984). Developmental neuropathology of organotin compounds. *Neurotoxicology*, **5**, 187–204.
- RICHTER-LANDSBERG, C. & BESSER, A. (1994). Effects of organotins on rat brain astrocytes in culture. *J. Neurochem.*, **63**, 2202–2209.
- RÖHL, C., GÜLDEN, M. & SEIBERT, H. (2001). Toxicity of organotin compounds in primary cultures of rat cortical astrocytes. *Cell Biol. Toxicol.*, **17**, 23–32.
- ROLFS, S., HAVERCAMP, W., BORGGREFE, W., MUSSHOF, U., ECKHARDT, L., MERGENTHALER, J., SNYDERS, D.J., PONGS, O., SPECKMANN, E.-J., BREITHARDT, G. & MADEJA, M. (2000). Effects of antiarrhythmic drugs on cloned cardiac voltage-gated potassium channels expressed in *Xenopus* oocytes. *Naunyn-Schmiedeberg's Arch. Pharmacol.*, **362**, 22–31.
- SAARY, M.J. & HOUSE, R.A. (2002). Preventable exposure to trimethyl tin chloride: a case report. *Occup. Med.*, **52**, 227–230.
- SCALLET, A.C., POTHULURI, N., ROUNTREE, R.L. & MATTHEWS, J.C. (2000). Quantitating silver-stained neurodegeneration: the neurotoxicity of trimethyltin (TMT) in aged rats. *J. Neurosci. Methods*, **98**, 69–76.
- SNOEIJ, N.J., PENNINKS, A.H. & SEINEN, W. (1987). Biological activity of organotin compounds – an overview. *Environ. Res.*, **44**, 335–353.
- STANTON, M.E., JENSEN, K.F. & PICKENS, C.V. (1991). Neonatal exposure to trimethyltin disrupts spatial delayed alternation learning in preweanling rats. *Neurotoxicol. Teratol.*, **13**, 525–530.
- STONER, H.B., BARNES, J.M. & DUFF, J.I. (1955). Studies on the toxicity of alkyl tin compounds. *Br. J. Pharmacol.*, **10**, 16–25.
- SWARTZWELDER, H.S., DYER, R.S., HOLOHAN, W. & MYERS, R.D. (1981). Activity changes in rats following acute trimethyltin exposure. *Neurotoxicology*, **2**, 589–594.
- SWARTZWELDER, H.S., HEPLER, J., HOLOHAN, W., KING, S.E., LEVERENZ, H.A., MILLER, P.A. & MYERS, R.D. (1982). Impaired maze performance in the rat caused by trimethyltin treatment: problem-solving deficits and perseveration. *Neurobehav. Toxicol. Teratol.*, **4**, 169–176.
- THAYER, J.S. (1995). Environmental Chemistry of the Heavy Elements: Hydrido and Organo Compounds. pp. 29–41. Weinheim: VCH Verlagsgesellschaft mbH.
- WALSH, T.J., MILLER, D.B. & DYER, R.S. (1982). Trimethyltin, a selective limbic system neurotoxicant, impairs radial arm-maze performance. *Neurobehav. Toxicol. Teratol.*, **4**, 177–183.

(Received July 27, 2004

Revised September 28, 2004

Accepted November 4, 2004)